Presented at the 2nd World Conference and Exhibition on Photovoltaic Solar Energy Conversion, Wien, July 1998

# VARIATIONS OF THE BACK SURFACE FIELD IN SILICON THIN-FILM SOLAR CELLS WITH INTERDIGITATED FRONT GRID

C. Hebling, S.W. Glunz, J. O. Schumacher, J. Knobloch
Fraunhofer Institute for Solar Energy Systems ISE, Oltmannsstr. 5, 79100 Freiburg, Germany
Phone: +49 (761) 4588-271, Fax: +49 (761) 4588-250, e-mail: christopher.hebling@ise.fhg.de

**ABSTRACT:** Crystalline Si Thin-Film Solar Cells (c-Si TFC) based on a silicon-on-insulator structure (SOI) were realized with an interdigitated front contact grid. Efficiencies of up to 19.2% on a 46µm thick silicon layer and 18.5% on a 30µm thick silicon layer were achieved. These layer systems were grown epitaxially on the 200nm thick seeding layer on top of an implanted compact $SiO_2$ intermediate layers. Various simulations were performed to study the influence of the back surface field (BSF) as well as of the grid finger distance and the finger width, respectively on the solar cell performance. It could be shown that the best results were obtained on thin (2µm) but very highly doped BSFs as well as on thick (8.5µm) and less highly doped BSFs. Solar cells with n-doped BSFs were much worse compared to $p^+$ BSFs. This might be a result of a lower crystallographic quality of the highly n-doped layers which act as seeding layers for the subsequent epi-growth. The finger-to-finger distance of the grid hardly affects the overall cell performance in a wide range, which is a promising result for a potential screen-printing process of an interdigitated front-grid in the future.
**Keywords:** Si-films-1: Back surface field-2: Simulation-3

## 1. INTRODUCTION

Front-contacted silicon thin-film solar cells on insulating substrates enable the utilization of the wide range of non-conducting or encapsulated impure substrate materials. Additionally, the possibility of a series interconnection of a string of electrically insulated cells on the same substrate exists since the p-busbar of one cell can be interconnected with the n-busbar of the next cell in order to realize this concept.

The potential of an interdigitated front grid applied on an epitaxially grown Si layer has been successfully demonstrated both for an SOI solar cell leading to efficiencies of up to 19.2% [1] as well as for a mini-module consisting of 24 cells of 1 $cm^2$ area all of which are placed on one 4"-wafer [2]. The mini-module achieved a $V_{oc}$ value of 15.2 V with the monolithical integration of the cells. Both results were obtained on layers which were prepared under ideal conditions in order to study the crucial parameters for this concept. It could be shown, for example, that a texturization step results in a $J_{sc}$ improvement of 3.5 mA due to the good reflection properties of the $SiO_2$ intermediate layer.

In addition to the optical confinement, recombination velocity at the rear surface ($S_{back}$) is another crucial parameter which can be influenced by a highly doped back $p^+$ region acting as a back surface field (BSF). From simulations and experimental results it is well known that effective surface recombination velocities of about 1000 cm $s^{-1}$ are sufficient for the front side, but back surface recombination velocities of even below 10 cm $s^{-1}$ can still improve the cell efficiency [3,4,5,6]. Thus, measures for achieving lowest $S_{back}$-values should be investigated and implemented.

With the above mentioned layer system, a solar cell efficiency of 19.2% (FF=77.5%, $V_{oc}$=668mV, $I_{sc}$=37.1mA) was achieved. In this cell, a 5µm thick $p^+$-layer with a boron concentration of $6x10^{18}$ $cm^{-3}$ acting as a BSF was included. However, cells with the same active layer thickness and quality but without a BSF reached only efficiencies of 16.8% (FF=78.1%, $V_{oc}$=634mV, $I_{sc}$=33.9mA). The corresponding spectral response measurements for cells with and without BSFs are shown in Fig.1. In these cells, the bulk diffusion length was several times larger than the epi-layer thickness ($L_{bulk} >> W_{epi}$). Therefore, with increasing cell thickness, the overall recombination is being reduced because the recombination at the rear side becomes less dominant.

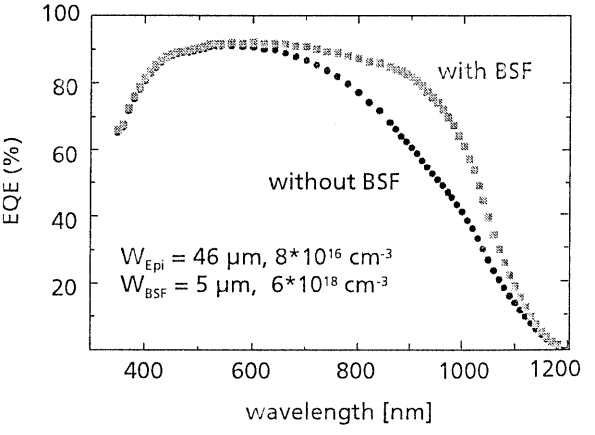


**Figure 1:** Spectral response measurements for two 46µm thick solar cells on a $SiO_2$ intermediate layer. The different behavior at long wavelengths arises from the highly doped $p^+$-layer acting as a BSF.

The aim of this paper is an experimental verification of the theoretical predictions of different BSF profiles when the $p^+$ thickness, the doping concentration and the doping type are varied. Furthermore, the distance between the p- and n- finger as well as the finger width were varied.

## 2. SIMULATIONS

Including all high temperature steps which occur during solar cell processing, the BSF-profiles were simulated with the numerical process simulator DIOS [7]. Additionally, spreading resistance measurements were performed in order to compare the simulated BSF-profiles with the real BSFs after cell processing. Figure 2 shows the profiles prior to and after cell processing (DIOS-simulation) and also one spreading resistance measurement for comparison.

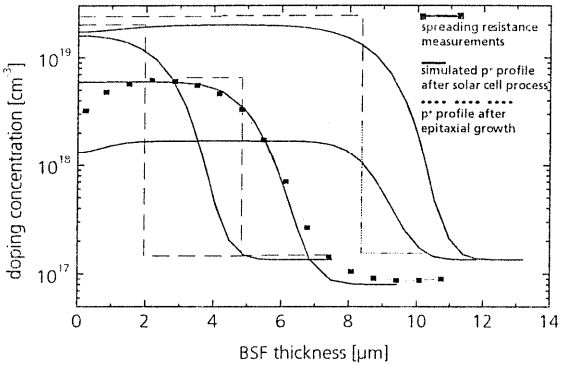


**Figure 2:** BSF-profiles after epi-growth and after cell processing (DIOS simulation). One spreading resistance measurement was performed in order to compare the simulations with the real doping concentration profile (squares).

The simulated BSF profiles were used as input files in order to perform 2-dimensional electrical calculations using the program DESSIS [7], as described in [6]. The symmetry element which was varied is shown on the right side of this column. The optical confinement of the cell structure resulting in the charge carrier generation profile was simulated with the 3-dimensional ray-tracing program RAYN [8]. The results of the BSF variations are shown in Fig. 3.

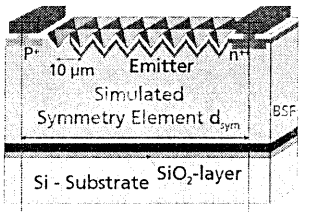


The results showed that the gains in $V_{OC}$ with a thicker $p^+$ layer are counterbalanced with the $I_{SC}$ losses due to higher recombination rates of carriers optically generated within the highly doped regions. The bulk diffusion length in the BSF was assumed to be limited only by Auger recombination. With this assumption, the electrical efficiency of the BSF is to a large extend independent of the BSF layer thickness. Nevertheless, the simulations predict a better performance with increased BSF-doping concentration.

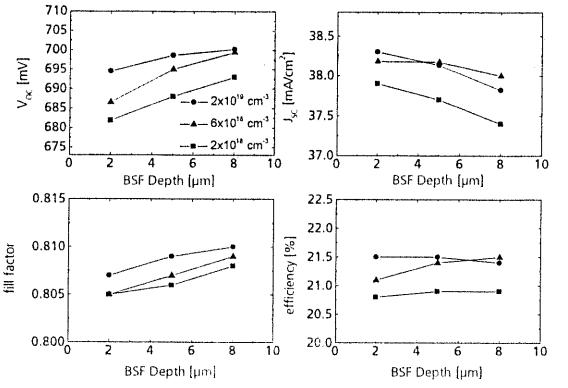


**Figure 3:** 2-dimensional simulations of the BSF in which the $p^+$ -doping concentration and the BSF layer thickness were varied.

## 3. EXPERIMENTAL

### 3.1 Variations of the back surface field

All layer systems were prepared on SOI substrates with an implanted insulating $SiO_2$ intermediate layer (SIMOX-wafer [9] with variations in the $p^+$-doping concentration ($1.7x10^{18}$ to $2\ 10^{19}$ $cm^{-3}$), the $p^+$ layer thickness (2µm to 8.5 µm), the epi-layer thickness (30 to 50µm) as well as the epi-layer doping concentration ($8x10^{16}$ $cm^{-3}$ and $1.35x10^{17}$ $cm^{-3}$). The layers were grown at IMEC in Leuven, Belgium, as well as at IMS in Stuttgart, Germany.

A new set of photolithographic masks was designed with three different n- to p-finger spacings (625µm, 715µm, 835µm) and with relaxed finger dimensions. The solar cell processing technology relies mainly on the process sequences which have been developed for the LBSF cells at Fraunhofer ISE [10] and which are also described in [1]. The main features are texturing with inverted pyramids, a double-step emitter, a local $p^+$-diffusion under the front base contacts, passivation of the surface with a high quality $SiO_2$ –layer, grid metallization with Ti/Pd/Ag and electroplating of the grid structure. The averaged solar cell results of three batches on the described layer systems are given in table 1.

| | No. cells | BSF [µm] | Dop. conc. [cm-3] | EPI [µm] | Voc [mV] | Jsc [mA] | FF [%] | Eta [%] |
|---|---|---|---|---|---|---|---|---|
| A | 4 | 5 | 6e18 | 50 | 634.4 | 35.1 | 75.1 | 16.7 |
| B | 4 | 5 | 6e18 | 40 | 641.1 | 35.2 | 73.2 | 16.9 |
| C | 4 | 5 | 6e18 | 30 | 653.2 | 35.4 | 75.3 | 17.3 |
| K | 8 | 2 | 2e19 | 45 | 653.3 | 33.3 | 78.7 | 16.9 |
| L | 8 | 8.5 | 2e19 | 45 | 650.1 | 32.2 | 79.6 | 16.6 |
| M | 8 | 8.5 | 1.7e18 | 45 | 651.9 | 33.2 | 78.5 | 16.9 |
| H | 4 | 3 | 6e18, n | 45 | 613.3 | 33.2 | 67.6 | 13.7 |
| J | 4 | 8 | 6e18, n | 45 | 609.2 | 32.0 | 70.1 | 13.6 |

**Table 1:** Averaged solar cell results (three solar cell batches) of the various layer systems. Samples A-C had different epi-layer thicknesses. Samples K-M had varying

BSF thicknesses and doping concentrations. Samples H and J were prepared with a non-connected n-doped layer (floating emitter).

The corresponding external quantum efficiency measurements are shown in Fig. 4 and 5.

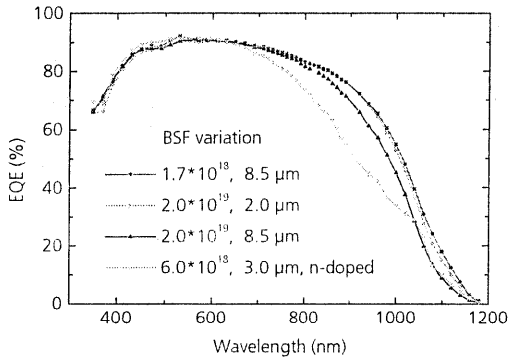


**Figure 4:** External quantum efficiency measurements with different BSFs varying in thickness and doping

As can be seen in Fig. 4, the rear surface passivation using a non-contacted $n^+$-layer resulted in quite a poor passivation quality. Best results were obtained for the thick lowly doped (8.5 µm, 1.7e18 $cm^{-3}$) and the thin highly doped BSF (2 µm, 2e19$cm^{-3}$). The passivation quality of the thick highly doped BSF (8.5µm, 2e19$cm^{-3}$) is somewhat worse. Assuming a very high bulk diffusion length in the epi-layer, maximum $S_{back}$-values of approximately 3500 cm/s for the first two BSFs (samples K, L) and 7500 cm/s for the latter one (sample M) can be determined. The Auger-limited diffusion length is 3.5 and 49 µm for a 2e19$cm^{-3}$ and 1.7e18$cm^{-3}$ doped layer, respectively. Thus, the first two BSFs are electrically transparent ($L_{BSF} > W_{BSF}$) while the thick highly doped is non-transparent. From this result it can be concluded that the $S_{SiO2}$ is of acceptable medium quality.

In a second experiment the thickness of the epi-layer was varied keeping the same BSF-parameters. The EQE measurements are given in Fig.5.

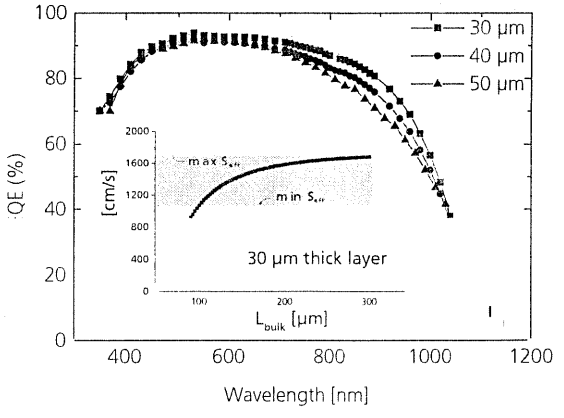


**Figure 5:** EQE-measurements for three different epi-layer thickness (30 – 50 µm, $N_A$=8x$10^{16}$$cm^{-3}$) and the same BSF parameters ($W_{BSF}$=5µm, $N_{BSF}$=6x$10^{18}$$cm^{-3}$).

From these measurements, $L_{eff}$ - values of 60µm, 88.5µm and 135µm were determined for 50µm, 40µm and 30µm thicknesses, respectively. This increase in $L_{eff}$ with decreasing epi-layer thickness means that the recombination in the bulk is still dominating the recombination at the rear surface. This is in contrast to the 10.2%.cell mentioned in the introduction. This experimental finding is also reflected in the open circuit voltages which were 634.4 mV 641 mV and 653 mV. Possible combinations of $S_{eff,back}$ and $L_{bulk}$ for the 30µm thick epi-layer thickness is given in Fig. 5 in the small graph. The $S_{eff}$-$L_{bulk}$ - combinations for the 30µm thick epi-layer thickness are evaluated from the internal quantum efficiency measurement.

An $S_{eff,max}$ (1700 cm/s) can be determined assuming a high bulk diffusion length of the 30µm thick epi-layer. A lower limit of $S_{eff}$ (1100 cm/s) can be calculated with an expression given in [11, 12], assuming a diffusion length which is only limited by Auger recombination.

### 3.2 Variations of the grid finger distance

Cells with three different n- to p-finger spacings (625µm, 715µm, 835µm) were prepared in order to verify the predictions from the simulations which were published in [1]. Furthermore, two grid finger widths (14µm and 28µm) were used to quantify the gains and losses according to reduced series resistance in a fine grid compared to higher shadowing losses for broad fingers. The results are given in Fig. 6.

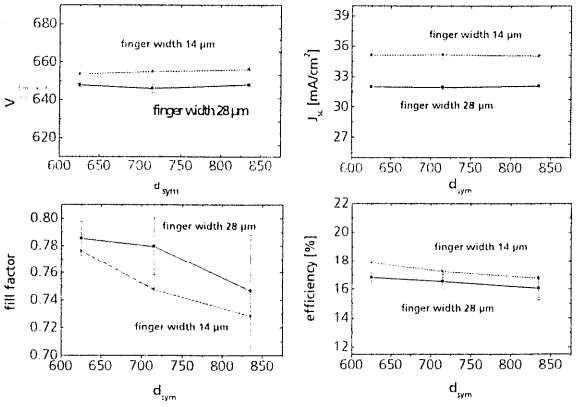


**Figure 6:** Averaged values of realized solar cells with three different p-finger to n-finger spacings and two different finger widths.

The difference in efficiency between the cells with a finger width of 14µm and 28µm was about 1% absolute. This small difference is due to the fact that the higher $V_{oc}$ and $J_{sc}$ values in the fine-grid cells are partly compensated by the higher series resistance which lead to a reduced fill factor. The dependence of the cell values on the finger-to-finger intervals is dominated by the fill factor losses with increasing distance between the fingers. This effect is reduced when grid fingers with larger diameters are used. The gains in $V_{oc}$ and $J_{sc}$ which were predicted in the simulations were not realized in all cells resulting in more or less equal average values.

## 4. CONCLUSIONS

The influence of different BSFs on the cell performance was studied by simulations and by realized solar cells made up of different layer systems. The best results were obtained with a thin highly doped BSF as well as a thick lowly doped BSF. From the realized cells, the crucial parameters were extracted and will contribute to improved modeling of thin film structures. The efficiency of solar cells with n-doped BSFs was measured to be about 4% absolute lower compared to $p^+$ BSFs. This is probably due to experimental difficulties in the n-layer growth since floating junctions were predicted to be as effective as $p^+$ layers. The epi-layer thickness variation revealed, that in this layer system, the main recombination activity occurs in the bulk. Thus, the better results were obtained with thinner layers which underlines the general benefit of silicon thin-film solar cells.

**Acknowledgments**

The authors would like to thank Guy Beaucarne and Jef Poortmans from IMEC for arranging for some of the epi-layer growths, B. Köster, C. Vorgrimler and T. Leimenstoll for cell processing and E. Schäffer for cell characterization.

This work was supported by the German Ministry for Education, Science, Research and Technology, BMBF and by the European Community. The authors are responsible for the content of this publication.

## REFERENCES

[1] C. Hebling, S. W. Glunz, J. O. Schumacher and J. Knobloch, "High Efficiency (19.2%) Silicon Thin-Film Solar Cells with Interdigitated Emitter and Base Front Contacts", in: Proc. 14th EC-PVSEC, Barcelona (1997) p.2318.

[2] S.W. Glunz, J. Knobloch, C. Hebling, W. Wettling, "The Range Of High-Efficiency Silicon Solar Cells Fabricated At Fraunhofer ISE", 26th IEEE PVSC, Anaheim, (1997) p. 231.

[3] H. Iwata, T. Ohzone, H. Takakura, "Numerical Simulation of Silicon-on-Insulator Thin-Film Solar Cells", Jpn. J. Appl. Phys. Vol. 34 (1995) p. 4055.

[4] H. Takato, T. Sekigawa, "Surface Passivation of Thin Silicon Solar Cells using Silicon-on Insulator Wafer", Jpn. J. Appl. Phys. Vol 34 (1995) p.6358.

[5] C. Hebling, R. Gaffke, S. Sterk, W. Warta, "Interdigitated Grid for Silicon Thin-Film Solar Cells on $SiO_2$-layers", 13th EC-PVSEC, Nice (1995) pp.1066-1069

[6] J.O. Schumacher, C. Hebling, W. Warta, "Analysis and design of a Thin Film Silicon Solar Cell on an Insulating Substrate", 14th EC-PVSEC, Barcelona, (1997) p.1467.

[7] Integrated Systems Engineering AG, Zurich, Switzerland, TCAD Release 4.1.1997.

[8] J.O. Schumacher, S. Sterk, B. Wagner, W. Warta, "Quantum Efficiency Analysis of High Efficiency Solar Cells with Textured Surfaces", 13th EC-PVSEC, Nice (1995).

[9] Gassel, H. Vogt, "SIMOX and 'Wafer Bonding: Combination of Competitors Complements One Another. In ECS Spring Meeting, Extended Abstracts, Proc. 93-1, S.1246-1247. The Electrochemical Society (1993).

[10] J. Knobloch, A. Noel, E. Schäffer, U. Schubert, F.J. Kamerewerd, S. Klußmann, W. Wettling, "High-Efficiency Solar Cells from FZ, Cz and Mc-Silicium Material", 23rd IEEE PVSC Louisville (1993), p.271.

[11] M.P. Godlewski, C.R. Baraona, and H.W. Brandhorst, "Low-high junction theory applied to solar cells", Solar Cells, **29** (1990) p.131.

[12] V. Henninger and W. Warta, "Analytical solution for charge carrier transients in a Two-Layer-Structure", 14th EC-PVSEC, vol 2, Barcelona (1997) p.2408.